Regular Article

PHYSICAL CHEMISTRY RESEARCH
Published by the
Iranian Chemical Society
www.physchemres.org
info@physchemres.org

***Phys. Chem. Res.**, Vol. 3, No. 3, 191-196, September 2015*
DOI: 10.22036/pcr.2015.9193

Synthesis and Characterization of α-Fe_2O_3 Nanoparticles by Simple Co-Precipitation Method

M. Farahmandjou* and F. Soflaee
Department of Physics, Varamin Pishva Branch, Islamis Azad University, Varamin, Iran
(Received 22 February 2015, Accepted 15 April 2015)

In the past decade, magnetic nanomaterials have attracted much attention due to their physical properties and technological applications. In this work, α-Fe_2O_3 nanoparticles were first synthesized *via* a simple co-precipitation method using iron chloride hexahydrate ($FeCl_3.6H_2O$) as precursor and ammonia solution as precipitator. The samples were then characterized by high resolution transmission electron microscopy (HRTEM), field effect scanning electron microscopy (FESEM), X-ray diffraction (XRD) and electron dispersive spectroscopy (EDS) Fourier transform infrared spectroscopy (FTIR) and UV-Vis spectrophotometer. XRD pattern showed that the iron oxide nanoparticles exhibited alpha-Fe_2O_3 (hematite) structure in nanocrystals. The α- Fe_2O_3 nano-powders with uniform size were prepared when the samples calcined at 500 °C, and the lowest particle size was found to be 30 nm by XRD technique and direct HRTEM observation. The surface morphological studies from SEM depicted sphere-like shaped particles with formation of clusters by increasing annealing temperature. The EDS spectrum showed peaks of iron and oxygen free of impurity with fewer elements. The sharp peaks in FTIR spectrum determined the purity of Fe_2O_3 nanoparticles and absorbance peak of UV-Vis spectrum showed the small bandgap energy of 2.58 ev.

Keywords: Iron oxide nanoparticles, Hematite, Co-precipitation, Synthesis

INTRODUCTION

Nanotechnology has large potential benefits to a range of areas. Nanomaterials have the potential to improve the environment through the development of new solutions to environmental problems. Nanotechniques have been touted as a new technology that may surpass the physical and chemical limitations of materials made from microparticles [1]. Recently, nanotechnology has attracted considerable interest in areas of biomedicine, such as cytotoxicity [2,3], drug delivery [4], biosensors [5], and magnetic resonance imaging [6], catalyst supporters [7], and biomedical applications, such as magnetic carriers for bioseparation [8], enzyme and protein immobilization [9] and contrast-enhancing media. Magnetic nanoparticles exhibit unique nanoscale properties and their utilization for various magnetic systems is of significant interest. Hematite (α-Fe_2O_3) is the most stable iron oxide and the most environmentally friendly semiconductor with Band gap energy of E_g = 2.1 eV [10]. It is traditionally used for red pigment [11], catalysts [12], electrodes [13], gas sensors [14,15], magnetic materials [16], photocatalytic [17] and anticorrosion protective paints. The properties of nano-powders greatly depend on their phase, microstructure and surface characteristics. The importance of iron oxide cannot be ignored as it is crucial for the accurate measurement of electricity and magnetism. In order to prepare homogenous nano-particles of iron oxide, researchers have employed in different routes to iron oxide nano-particles such as sol-gel processes [18], w/o microemulsion [19], combustion [20], solvothermal [21], hydrothermal [22], precursor [23],

*Corresponding author. E-mail: farahmandjou@iauvaramin.ac.ir

solvent evaporation *etc*. However, these methods usually involve special equipment, high temperatures, and the tedious removal of impurities, which are all time-consuming and come at a high monetary cost. The co-precipitation process has been used for the preparation of nano or sub-micro powders in a variety of metal oxides using inorganic salts as precursors [24]. The synthesis of magnetite nanoparticles with controlled size has long been of scientific and technological interest. However, uniform physical and chemical properties of magnetite nanoparticles greatly depend upon the synthesis route, and how to develop a simplistic and effective way to synthesize magnetite particles with high dispersion and narrow size distribution remains a challenge. There are two well-known crystalline types of Fe_2O_3: maghemite (the γ-phase) with cubic structure and hematite (the α-phase) with rhombohedral structure. The phase transition of γ → α-Fe2O3 takes place during calcination at about 400 °C [25]. The phase transformation which occurs during calcination gives rise to transform α-Fe_2O_3 powder which has undergone considerable aggregation and grain growth [26,27]. In this paper, ferric oxide nanorods were synthesized by co-precipitation route using iron chloride precursor. Structural and surface morphological properties are discussed by XRD, HRTEM, FESEM, FTIR, UV-Vis and EDS analyses.

Experimental Detail

All chemicals were of analytical grade and were used as received without further purification. Iron oxide nanoparticles were synthesized by a simple co-precipitation synthesis according to the following manner. Firstly, 10 g of $FeCl_3.6H_2O$ was dissolved in 150 ml pure water with stirring at room temperature. A 2 ml NH_4OH solution was then added drop wise (drop rate = 1 ml min^{-1}) to the stirring mixture at room temperature. The Ph = 1 was maintained during the synthesis. The resulting black dispersion was continuously stirred for 1 h at room temperature and then heated to evaporate for 2 h at 80 °C to yield a brown powder. The product were cooled to room temperature and finally calcined at 500 °C for 4 h. For all samples, analyses were done without any washing and purification.

The specification of the size, structure and surface morphological properties of the as-synthesis and annealed Fe_2O_3 nanoparticles were carried out. X-Ray diffractometer

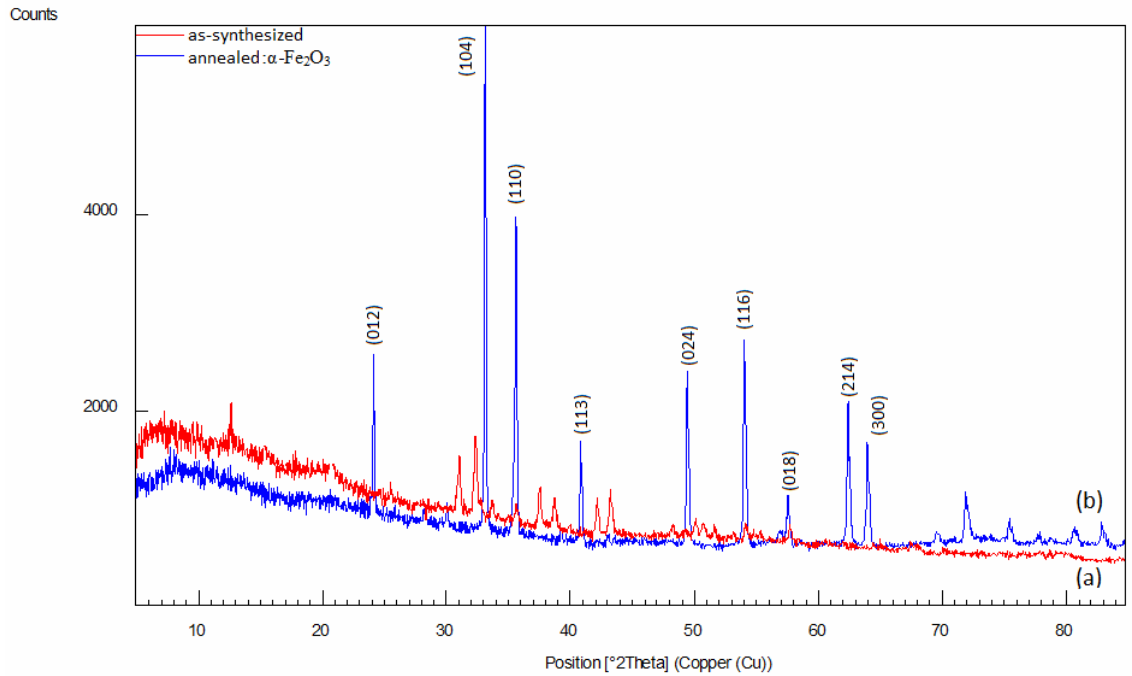

Fig. 1. XRD pattern of iron oxide nanoparticles (a) before and (b) after annealing.

(XRD) was used to identify the crystalline phase and to estimate the crystalline size. The XRD pattern were recorded with 2θ in the range of 4-85^o with type X-Pert Pro MPD, Cu-K_α: λ = 1.54 Å. The morphology was characterized by field emission scanning electron microscopy (SEM) with type KYKY-EM3200, 25 kV and transmission electron microscopy (TEM) with type Zeiss EM-900, 80 kV. The Fe and O elemental analysis of the samples was performed by energy dispersive spectroscopy (EDS) type VEGA, 15 kV. All the measurements were carried out at room temperature.

RESULT AND DISCUSSION

X-rar diffraction (XRD) at 40 Kv was used to identify crystalline phases and to estimate the crystalline sizes. Figure 1 shows the X-ray diffraction patterns of the powder of the nanoparticles. Figure 1a shows the XRD pattern of the sample before annealing and Fig. 1b shows the XRD pattern of the sample after heat treatment. A γ → α-Fe_2O_3 phase transformation took place during calcination between 300 and 400 °C. An abrupt increase in the amount of a phase occurred when the calcinations temperature rose above 400 °C. The α-Fe_2O_3 phase was the only phase present for the powder calcined above 500 °C. The exhibited picks correspond to the (012), (104), (110), (113), (024), (116), (018), (214) and (300) of a rhombohedral structure of α-Fe_2O_3 is identified using the standard data. The mean size of the ordered Fe_2O_3 nanoparticles has been estimated from full width at half maximum (FWHM) and Debye-Sherrer formula according to equation the following:

$$D = \frac{0.89\lambda}{B\cos\theta} \quad (1)$$

where, 0.89 is the shape factor, λ is the x-ray wavelength, B is the line broadening at half the maximum intensity (FWHM) in radians, and θ is the Bragg angle. The mean size of annealed α-Fe_2O_3 nanoparticles was around 30 nm from this Debye-Sherrer equation. The lattice constant so obtained for alpha Fe_2O_3 nanoparticles were a = b = 5.0342 A^o and c = 13.74650 A^o.

Surface morphology of the as-synthesis and calcined samples was studied using SEM analysis. Figure 2 shows

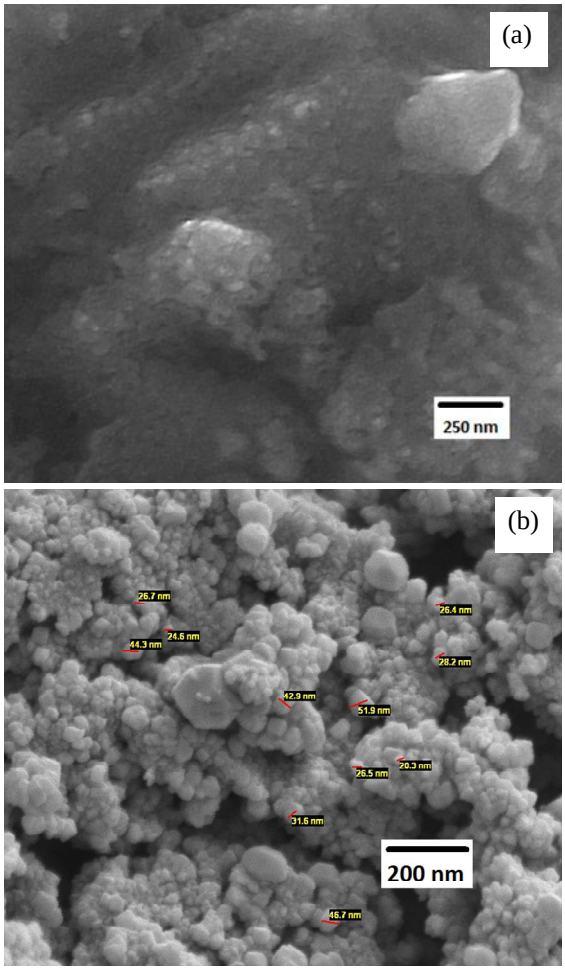

Fig. 2. SEM images of the Fe_2O_3 nanoparticles: (a) as prepared; (b) annealed sample

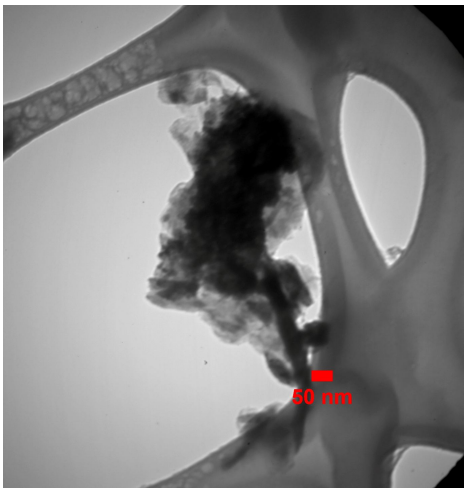

Fig. 3. TEM image of the as-prepared Fe_2O_3 nanoparticles

the SEM images of the as-prepared and annealed Fe_2O_3 nanoparticles. Figure 2a shows the SEM image of the as-prepared Fe_2O_3 nanoparticles prepared by co-precipitation method. In this figure, the particles prepared with formation of clusters. Figure 2b shows the SEM image of the annealed Fe_2O_3 nanoparticles at 500 °C for 4 h. The Fe_2O_3 nanocrystals formed were agglomerated. These analyses show that high crystallinity emerged in the samples surface by increasing annealing temperature. With increasing temperature the morphology of the particles changes to the sphere-like shaped and nanopowders were less agglomerated. The particle size of as-prepared Fe_2O_3 nanoparticles were measured about 20 nm and the particle size of annealed Fe_2O_3 nanoparticles were measured about 30 nm in diameter. As you can see the particles were crystallized as polyhedron after heat treatment.

Average particle size of the as-prepared powders was measured by using high resolution TEM. The transmission electron microscopic analysis was carried out to confirm their growth pattern and the distribution of the crystallites. Figure 3 shows the as-synthesized TEM image of plate-like shaped Fe_2O_3 nanoparticles prepared by chemical precipitation route. It can be seen that nanorods were prepared with less aggregation.

Energy dispersive spectroscopy (EDS) of Fe_2O_3 prepared by co-precipitation is shown in Fig. 4 which confirms the existence of Fe and O with weight percent. EDS was used to analyze the chemical composition of a material under SEM. EDS shows the peaks of iron and oxygen with fewer chlorine elements. As it can be seen the green peaks is related to chlorine elements which they have not been removed from the samples. Because the samples were not purified and centrifuged before they analyzed by EDS.

According to Fig. 5, the infrared spectrum (FTIR) of the synthesized Fe_2O_3 nanoparticles was in the range of 400-4000 cm^{-1} wavenumber which identify the chemical bonds as well as functional groups in the compound. The large broad band at 3398 cm^{-1} is ascribed to the O-H stretching vibration in OH^- groups. The absorption picks around 1604 cm^{-1}, 1487 cm^{-1} are due to the asymmetric and symmetric bending vibration of C=O. The strong band below 700 cm^{-1} is assigned Fe-O stretching mode. The band corresponding to Fe-O stretching mode of Fe_2O_3 is seen at 576 cm^{-1}.

UV-Vis absorption spectral study may be assisted in understanding electronic structure of the optical band gap of the material. Absorption in the near ultraviolet region arises from electronic transitions associated within the sample.

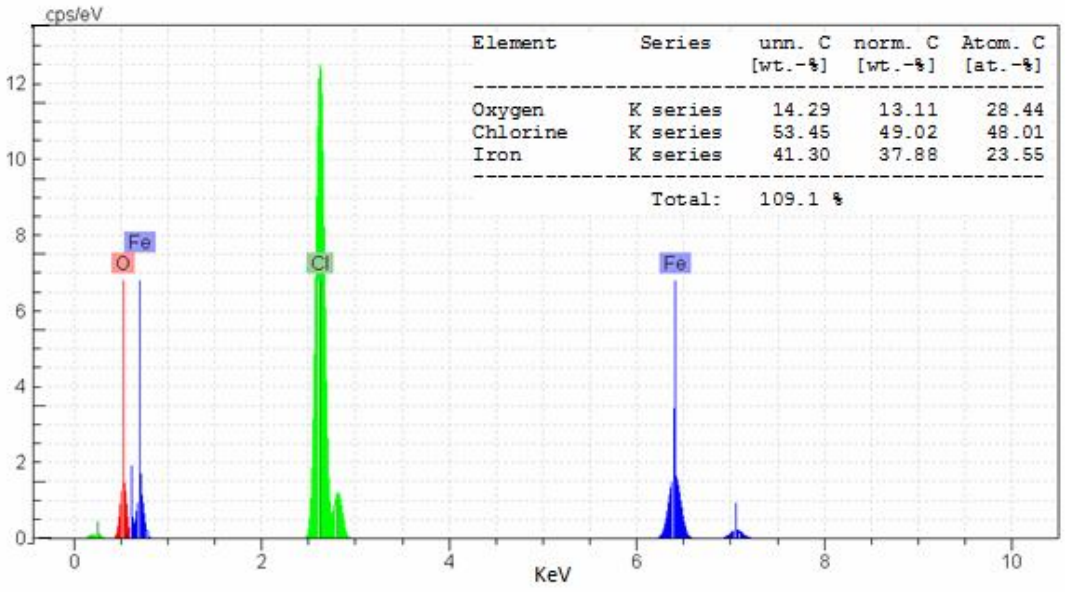

Fig. 4. EDS spectra of the as-synthesized Fe_2O_3 prepared by wet synthesis.

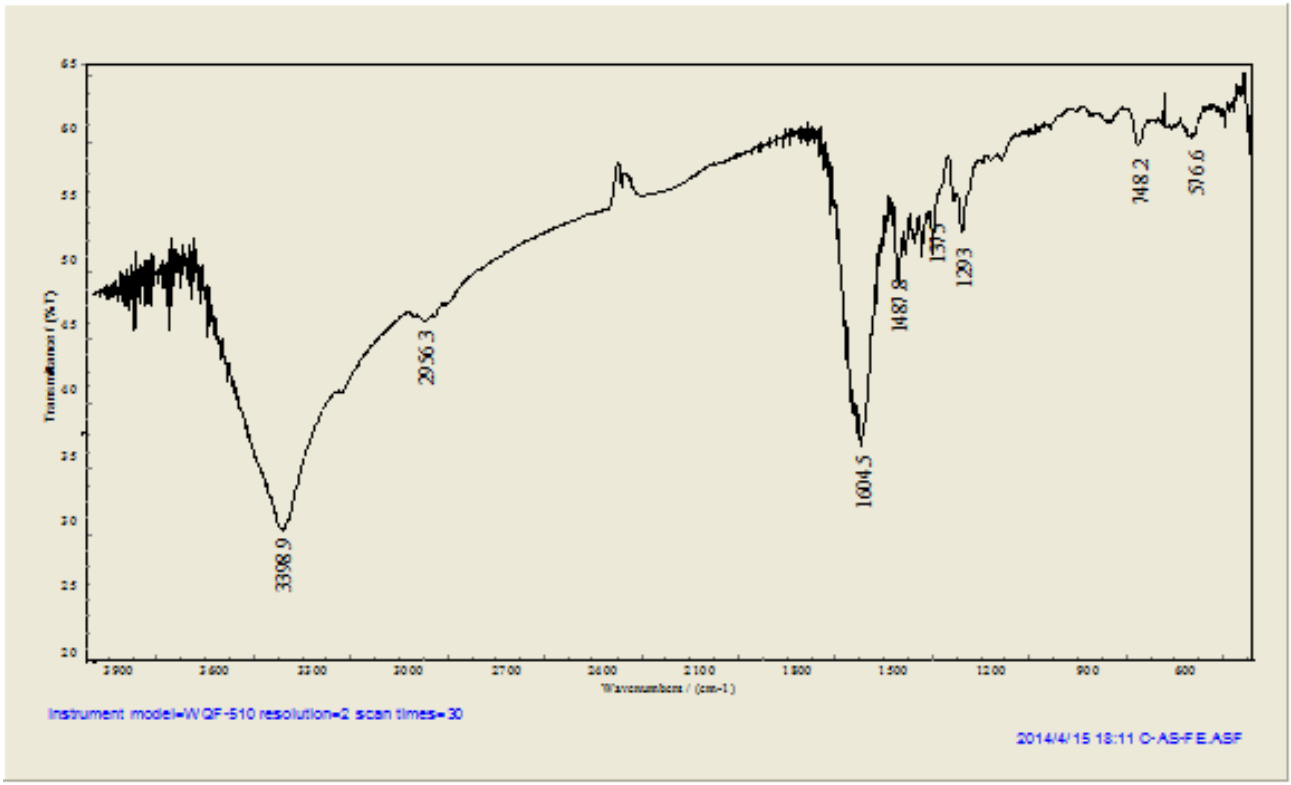

Fig. 5. FTIR spectrum of Fe_2O_3 sample.

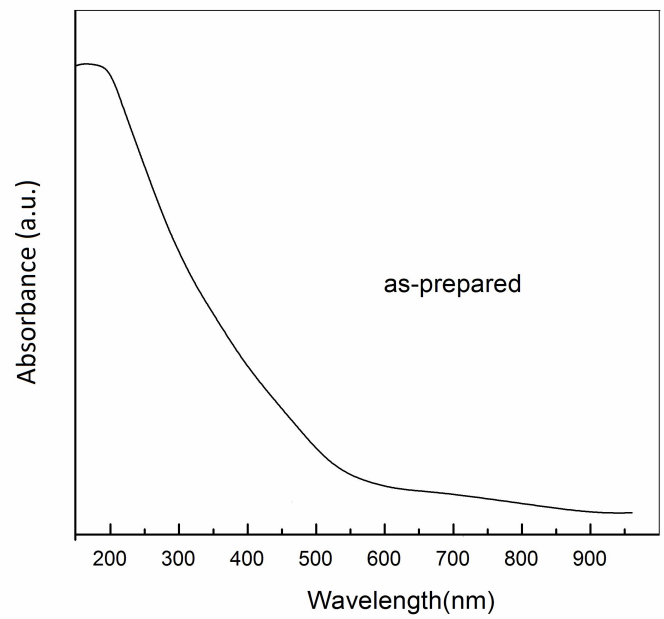

Fig. 6. UV-Vis absorption spectra of as-prepared Fe_2O_3 nanoparticles.

UV-Vis absorption spectra of as-prepared and annealed Fe_2O_3 nanoparticles are shown in Fig. 6. The small bandgap energy of 2.58 ev were achieved at wavelength near 480 nm for as-synthesized Fe_2O_3 samples.

CONCLUSIONS

Simple co-precipitation synthesis has been successfully carried out to fabricate α-Fe_2O_3 nanopowders at a relatively low temperature. XRD spectrum shows rhombohedral (hexagonal) structure of α-Fe_2O_3. From SEM images, it is clear that with increasing temperature the morphology of the particles changes from plate-like shaped to sphere-like shaped and nanopowders were less agglomerate. TEM image exhibits that the as-synthesized Fe_2O_3 nanorods prepared by co-precipitation route with an average diameter about 30 nm with less aggregation. EDS shows only peaks of iron and oxygen and indicates the absence of impurities in prepared Fe_2O_3. FTIR data, showed the presence of Fe-O stretching mode of Fe_2O_3. The UV-Vis absorption of iron oxide nanoparticles showed a strong pick at 480 nm with direct small band of 2.58 eV.

ACKNOWLEDGMENTS

The authors are thankful for the financial support of varamin pishva branch at Islamic Azad University for analysis and the discussions on the results.

REFERENCES

[1] M.Y. Masoomi, G. Mahmoudi, A. Morsali, J. Coordination Chem. 63 (2010) 1186.

[2] M. Morales, S. Veintemillas-Verdaguer, C. Serna, J. Mater. Res. 14 (1999) 3066.

[3] A.Villanueva, M. Cañete, Nanotechnology 20 (2009) 115103.

[4] A. Tomitaka, A. Hirukawa, T. Yamada, J. Magn. Magn. Mater. 321 (2009) 1482.

[5] P.C. Morais, V.K. Garg, A.C. Oliveira, Hyperfine Interact. 190 (2009) 87.

[6] M. Varshney, Y. Li, Biosens. Bioelectron 22 (2007) 240824.

[7] J.M. Perez, L. Josephson, T.O. Loughlin, D. H Lgemann, R. Weissleder, Nat. Biotechnol. 20 (2002) 816.

[8] T.J. Yoon, W. Lee, Y.S. Oh, J.K. Lee, New J. Chem. 27 (2003) 227.

[9] P.S. Doyle, J. Bibette, A. Bancaud, J. Viovy, Science 295 (2002) 2237.

[10] D. Cao, P. He, N. Hu, Analyst 128 (2003) 1268.

[11] X.G. Wen, S.H. Wang, Y. Ding, Z.L. Wang, S.H. Yang, J. Phys. Chem. B 109 (2005) 215.

[12] C. Feldmann, Adv. Mater. 13 (2001) 1301.

[13] A.T. Bell, Science 299 (2003) 1688.

[14] S.S. Yarahmadi, A.A. Tahir, B. Vaidhyanathan, K.G.U. Wijayantha, Mater. Lett. 63 (2009) 523.

[15] Y. Wang, J.L. Cao, S.R. Wang, X.Z. Guo, J. Zhang, H.J. Xia, J. Phys. Chem. C 112 (2008) 17804.

[16] G. Neri, A. Bonavita, S. Galvagno, P. Siciliano, S. Capone, Sens Acturators B 82 (2002) 40.

[17] Z.H. Jing, S.H. Wu, Mater. Chem. Phys. 92 (2005) 600.

[18] Z.H. Zhang, M.F. Hossain, T. Takahashi, Appl. Catal. B Environ. 95 (2010) 423.

[19] X.Q. Liu, S.W. Tao, Y.S. Shen, Sens Actuators B 40 (1997) 161.

[20] A.B. Chin, I.I. Yaacob, J. Mater. Process Tech. 191 (2007) 235.

[21] S.U. Sonavane, M.B. Gawande, S.S. Deshpande, A. Venkataraman, R.V. Jayaram, Catal. Commun. 8 (2007) 1803.

[22] S. Chaianansutcharit, O. Mekasuwandumrong, P. Praserthdam, Ceram. Int. 33 (2007) 697.

[23] C.Q. Hu, Z.H. Gao, X.R. Yang, Mater. Chem. Phys. 104 (2007) 429.

[24] J. Rockenberger, E.C. Scher, A.P. Alivisatos, J. Am. Chem. Soc. 121 (1999) 11595.

[25] B. Wang, Q. Wei, S. Qu, Int. J. Electrochem. Sci. 8 (2013) 3786.

[26] J. Morales, J.L. Tirado, C. Valera, J. Am. Ceram. Soc. 72 (1989) 1244.

[27] W. Feitknecht, U. Mannweiler, Helv. Chim. Acta 50 (1967) 570.

[28] H. El Ghandoor, H.M. Zidan, M.H. Khalil, M.I. M. Ismail, Int. J. Electrochem. Sci. 7 (2012) 5734.